CrossMark

ORIGINAL PAPER

Polystyrene/hydrophobic TiO$_2$ nanobelts as a novel packaging material

Mona H. Abdel Rehim[1] · Ahmed M. Youssef[1] · Ahmed Ghanem[1]

Abstract Titanium oxide nanobelts (TiO$_2$ NBs) are successfully prepared by hydrothermal method in alkaline medium. The surfaces of the obtained NBs were modified to become hydrophobic character. Commercial polystyrene was loaded with different ratios of the aforementioned hydrophobic TiO$_2$ NBs. The casted films were characterized using thermal gravimetric analysis (TGA) and mechanical testing, and their morphology was studied by TEM. The mechanical properties of the prepared PS/TiO$_2$ NBs composite were evaluated and found to be enhanced by increasing the loading of TiO$_2$ NBs. Correspondingly, the antibacterial testing was performed against representative strains of Gram-positive and Gram-negative bacteria. The results showed that the prepared nanocomposite can be used as packaging materials.

Keywords Polystyrene · TiO$_2$ nanobelts · Antibacterial properties · Packaging material

Introduction

Hybridization of polymers with inorganic materials is widely utilized to combine the dissimilar properties of organic and inorganic materials [1–3]. Various techniques have been used for the preparation of polymer hybrids, such as emulsion polymerization [4], layer-by-layer (LBL) method [5] sol–gel method [6], blending and grafting [7, 8]. Polystyrene is characterized by a unique combination of properties such as being extremely strong yet light weight, economic, ease of processing and provides excellent insulation. It finds applications in toys, house

✉ Mona H. Abdel Rehim
  monaabdelrehim23@gmail.com

1 Packing and Packaging Materials Department, National Research Centre, Elbehous Street, Dokki, Giza 12622, Egypt

wares and electronic appliances. Moreover, it is widely used as food packaging material. Nevertheless, the polymer can be contaminated with microorganisms or invaded by bacteria that cause deterioration of the food stuff. Modification of polystyrene with TiO_2 as antibacterial agent mostly during the melt compounding was investigated [9, 10]. The antibacterial reactivity of TiO_2 originated from the high reactivity of the excited hydroxyl radicals present on its surface. It was reported that smaller semiconductor particles will increase the surface area and the catalytic effect [11]. Therefore, TiO_2 nanoparticles have better antibacterial activity than micron-sized particles. Recently, introduction of TiO_2 nanorods into polystyrene matrix by mixing pre-synthesized oleic acid capped colloidal TiO_2 nanorods into commercial polystyrene via solvent blending using chloroform was reported [12]. It was found that the surfactant plays an important role for interactions between the polymer and the filler.

In this study, we present novel polystyrene/modified TiO_2 composite (PS/M-TiO_2 NBs) with excellent antibacterial properties. The newly modification method of TiO_2 NBs with poly(vinyl benzyl chloride) (or pVBC) offered the nanobelts hydrophobic character which enhanced their dispersion in the polystyrene matrix.

Experimental part

Materials

Titanium dioxide (TiO_2) with cross-sectional dimension about 25 nm was obtained from Degussa. Sodium chloride (99 %) and sodium hydroxide-(98 %) were purchased from Honeywell, Germany and Macron Chemicals, Sweden, respectively. 4-Vinyl benzyl chloride (VBC) monomer was obtained from Across Organics (Tech. grade, 90 %) and purified using sodium hydroxide to remove the free-radical inhibitor. Commercial Polystyrene (PS) was obtained from CHIMEI Corporation; Taiwan Benzoyl Peroxide (98 %) was a product of Alpha Chemicals. Calcium Carbonate (98.5 %) was purchased from OXFORD laboratory. All the used solvents such as toluene (99.8 %, M-TEDIA), methanol (99 %, ADWIC) and methylene chloride (99.5 %, TEDIA) were used as received unless otherwise noted.

Techniques

The structure and surface morphology of the prepared nanocomposites were examined using JEOL JEM-1230 transmission electron microscope (TEM) with acceleration voltage of about 80 kV and JEOL-SEM scanning electron microscope (SEM), respectively. XRD patterns were recorded by Diano X-ray diffractometer with Cu Kα-radiation source energized at 45 kV. The thermal behavior was studied using Simultaneous DSC-TGA instrument or SDT Q600 under nitrogen atmosphere at heating rate of 10 °C/min. Mechanical properties were evaluated using ASTM D 638 Tensile tests on plastics.

Methods

Preparation of titanate nanowires

In a typical procedure, 0.2 g of titanium nanoparticles (P25) in strong alkaline aqueous solution of NaOH (10 M, 40 ml) was placed into a Teflon-lined autoclave. The mixture was stirred to form a milky suspension, sealed and hydrothermally treated at 220–270 °C for 3 days. The precipitate formed was separated by filtration and washed with de-ionized water until a pH value near 8 was reached. Up to this stage, the precipitate was denoted hydrogen form $Na_xH_{2-x}Ti_3O_7$ ($x = 0.75$). Straightforward, the precipitate was immersed in an aqueous solution of sodium chloride (10 M) for 72 h to replace the hydrogen with sodium through cation exchange and finally gain the sodium form, $Na_2Ti_3O_7$. The sample was then oven dried at 80 °C overnight. It should be stressed that the key factor for producing pure titanate nanobelts is the optimization of NaOH concentration of along with the time of hydrothermal treatment.

Surface modification of TiO_2 NBs

Modification of NWs surface was carried out through in situ polymerization of VBC monomer in the presence of the TiO_2 NBs to obtain p(VBC)/$Na_2Ti_3O_7$ nanocomposites. The detailed method is reported recently (Ghanem et al. [13]) as follows: 1.7 ml of VBC, 0.5 g of the $Na_2Ti_3O_7$-NBs, and 15 ml toluene were mixed under N_2. The mixture was sonicated for 30 min and stirred (5000 rpm) for 72 h. 0.04 g of benzoyl peroxide was added to the mixture, and the polymerization reaction was carried out at 95 °C for an hour. The resulting nanocomposite was precipitated in 200 mL methanol and re-dissolved again in toluene for 3 times, then washed with distilled water several times. Finally, the formed surface-modified TiO_2 NBs obtained in the form of pVBC/$Na_2Ti_3O_7$-NBs nanocomposite was dried at 70 °C under vacuum overnight.

Preparation of PS/M-TiO_2 NBs composites

PS nanocomposites were prepared through mixing the desired amount of PS polymer dissolved in 100 ml toluene, with different concentrations of M-TiO2 NBs (3, 6, 9 and 12 %). The mixtures were stirred for 3 h at room temperature, and then the dispersion solutions were casted into Petri dishes and dried in an oven at 60 °C.

Antimicrobial activity (agar plate method)

The agar plate method was taken to evaluate the antimicrobial activities of microbial extract and/or pure compounds compared with the positive (plates having discs containing solvent only) and negative controls (plates containing test microbe only). This disc diffusion test has been done according to Collins and Lyne [14]. The antimicrobial activities of the films were tested against four strains of microorganism, i.e., *Staphylococcus aureus* (Gram-positve bacteria), *Pseudomonas*

aeruginosa (Gram-negative bacteria), *Candida albicans* (yeast) and *Aspergillus niger* (fungi). Both bacterial and yeast test microbes were grown on nutrient agar (DSMZ1) medium (g/l): beef extract (3), peptone (10), and agar (20). On the other hand, the fungal strain was grown on Czapek-Dox (DSMZ 130) medium (g/l): sucrose (30), $NaNO_3$ (3), $MgSO_4 \cdot 7H_2O$ (0.5), KCl (0.5), $FeSO_4 \cdot 7H_2O$ (0.001), K_2HPO_4 (1) and agar (20). The culture of each microorganism was diluted with sterile distilled water to 10^7 to 10^8 CFU/ml. Sample (film) discs (5 mm $\varnothing$ diameter) were located on the surface of the agar plates (10 cm diameter containing 25 ml of solidified media. The discs were placed on inoculated agar plats and incubated for 24 h (yeast and bacteria) at 37 °C (bacteria) and 48 h (fungi) at 30 °C (fungi and yeast).

Results and discussion

Alkaline hydrothermal method is used to prepare TiO_2 nanobelts whose morphology was investigated by SEM and shown in Fig. 1a. The image reveals the copious quantity of the nanobelts with obvious separation between them, i.e., no aggregated bundles. Figure 1b shows the TEM of an isolated nanobelt and confirms that the successful synthesis of the TiO_2 nanobelt is achieved without defects.

It is worth to mention that the growth mechanism of TiO_2 nanobelts is still not exactly known, but it is believed that NaOH might act as soft template during formation of the nanobelts. Moreover, temperature is crucial factor, for example, at low temperature (110 °C) [15], because of the limited growth of TiO_2 particles, the layered structures were very thin, and could easily be rolled up into tubular structures. While in our work, the high temperature and long experiment time allowed thick layered structures to be formed and rolled into the as-shown nanobelts with about 50 nm diameter.
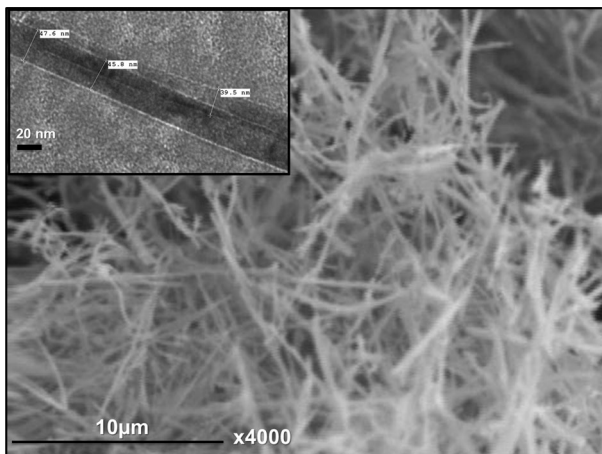

Fig. 1 SEM image of TiO_2 NBs ($Na_2Ti_3O_7$) and *inset* TEM of a single belt

XRD pattern for the unmodified TiO_2 nanobelts which has the formula $Na_2Ti_3O_7$ and the spectrum of the modified form $Na_2Ti_3O_7$/p(VBC) are shown in Fig. 2. The spectrum of unmodified nanobelts reveals the presence of monoclinic $Na_2Ti_3O_7$ phase [$2\theta = 10.5°$ (100), 25.7° (110) and 29.7° (003)]. Formation of the $Na_2Ti_3O_7$/p(VBC) nanocomposite by in situ polymerization technique has lead to shift in the main peak of TiO_2 to $2\theta = 11$. Moreover, a new form was obtained with the formula Ti_3O_5.

The morphology study of the hydrophobic TiO_2 nanobelts carried out by SEM, reveals the complete surface coverage of the nanobelts with the polymeric modifier (Fig. 3). It is worth to mention that, through the experimental procedures, NBs were stirred with the monomer for 3 days, which might lead to shortening of the NBs than the original as can be observed. Nevertheless, the relatively smooth coating on the Na-intercalated NBs is in line with the ionic interaction between chloride anions of the polymer and sodium cations present on the TiO_2 MB's.

Formation of polystyrene/M-TiO_2 NBs

Casted films of polystyrene/M-TiO_2 NBs were prepared through blending different amounts of the M-TiO_2 NBs with commercial polystyrene solution. The obtained films showed high homogeneity with no noticeable aggregates. However, careful inspection of a well-separated M-TiO_2 NBs in composite sample with HR TEM reveals the NBs retained their shape after several steps of modification and composite preparation (Fig. 4). The image showed that the diameter of the modified TiO_2 NBs ranged from 0.3 till 0.8 µm.

Thermal stability of PS/M-TiO_2 NBs composites was studied using thermal gravimetric analysis (Fig. 5). The thermogram shows the weight loss curves for three modified polystyrene samples compared to blank polystyrene. It can be
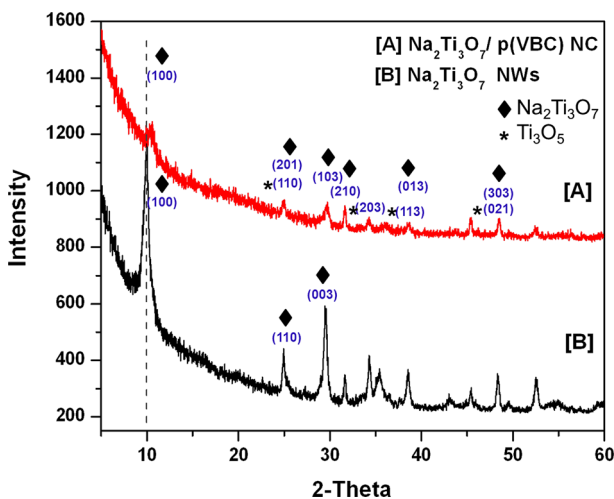
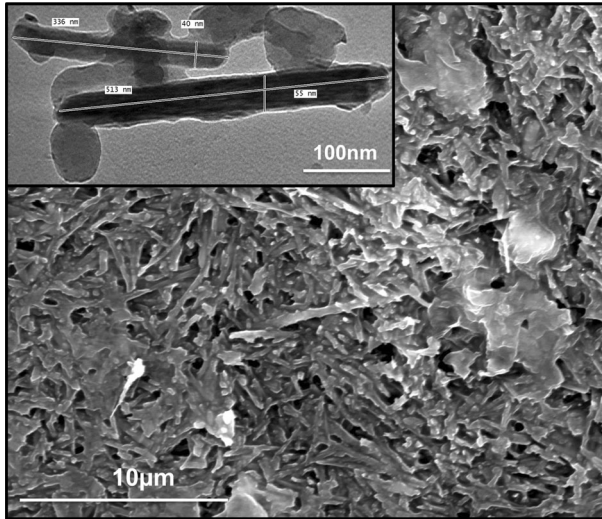**Fig. 2** XRD patterns of TiO_2 NBs and its nanocomposite p(VBC)/$Na_2Ti_3O_7$

Fig. 3 SEM image of modified TiO$_2$ NBs (p(VBC)/Na$_2$Ti$_3$O$_7$ nanocomposites and inset TEM of a single belt nanocomposite
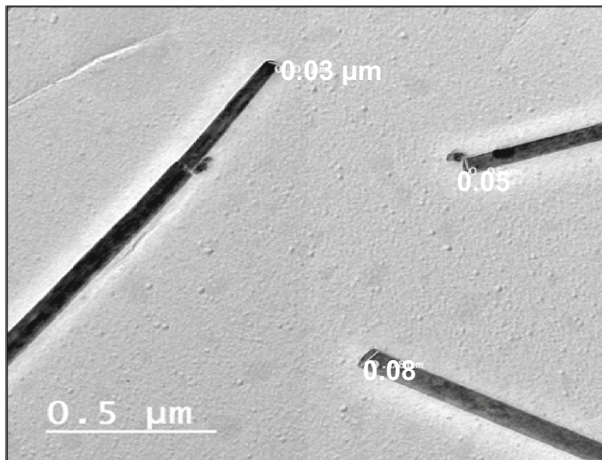

Fig. 4 HR-TEM of PS-M-TiO$_2$ NBs (6 % loaded sample)

noticed that while blank polystyrene showed one step with onset at 217 °C, the loaded polystyrene samples showed thermograms with two weight loss steps. The first step ended by 10 % weight loss which occurred at temperature 112 °C and can be attributed to losing of rest solvents present in the composite samples. The second step starts at 255 °C which can be due to the degradation of polymer backbone. So, generally speaking, the prepared modified polystyrene composite is more thermally stable than the blank polymer.
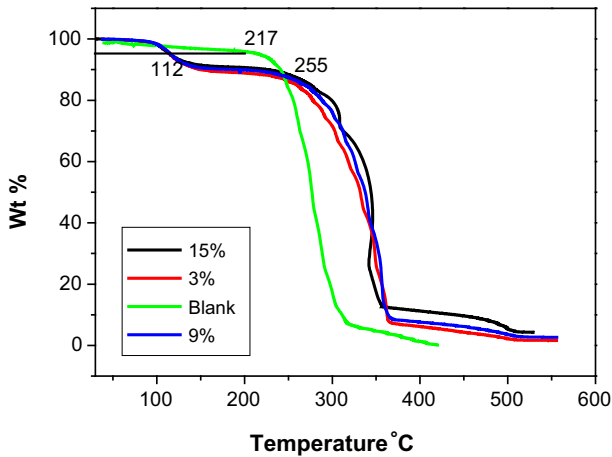
Fig. 5 TGA thermogram of PS/M-TiO$_2$ NBs

Table 1 Mechanical properties of PS/M-TiO$_2$ composites

Sample	Tensile strength (kg/cm^2)	Elongation at break (kg/cm^2)
Blank	66.13	56.00
3 %	97.97	90.31
6 %	111.87	106.12
9 %	118.32	107.45
12 %	112.29	127.97

It is worth to point out that the addition of 3 % of the hydrophobic TiO$_2$ NBs to PS matrix increased degradation temperature of the formed composite. On the other hand, by increasing the loading amount, thermal degradation temperature is decreased as a direct effect for the photoactivity of TiO$_2$; this behavior is consistent with that reported in the literature survey and rationalizes the lack of change in the thermal degradation for the obtained composites with higher loadings.

Mechanical properties

The tensile experiment is the most common mechanical test that reveals several significant mechanical properties, such as modulus of elasticity, yield strength, ultimate tensile strength, ductility, and toughness. The tensile instrument elongates the sample at a constant rate, measures continuously and records the applied load and elongation of the sample. Through the stretching of the sample, changes happen in its physical dimensions and its mechanical properties. Table 1 demonstrates that the mechanical properties of the prepared polystyrene nanocomposites based on the modified TiO$_2$ NBs were increased by increasing the loaded amounts by the following ratios (3, 6, 9 and 12 %) based on polystyrene matrix. The maximum Fσ M was increased from 66.13 kg/cm^2 for the blank polystyrene to reach 118.32 kg/

cm^2 when increasing the concentration of modified TiO_2 nanobelts to 9 %, then start to decrease to 112.29 kg/cm^2 by increasing the concentration of modified TiO_2 nanobelts. This result can be attributed to the fact that at low concentrations of TiO_2 NBs, good interfacial adhesion is formed. This allows the interfacial structure of the nanocomposite to bear part of the tensile strength [16]. By increasing the amount of modified TiO_2 NBs in the polymer matrix, agglomerates start to appear and cause microcracks in the nanocomposites and hence reduce tensile strength. Correspondingly, elongation at break was raised to be 127.97 kg/cm^2 by increasing concentration of modified TiO_2 in the nanocomposites films (12 % loading) compared with pure polystyrene film which showed elongation at break of 56.00 kg/cm^2.

Antimicrobial activity of the prepared PS/modified TiO_2 nanocomposites

Inorganic antibacterial nanomaterials were commonly in the form of a nanocomposite which is considered as extremely safe (non-volatile) complementary to organic materials. Metallic ions having antibacterial and antifungal abilities, such as Ag and TiO_2 nanoparticles, are impregnated in a mineral or mixed with a carrier to form the nanocomposite or practical as a coating. The particular high reactivity of metal nanoparticles is associated with known and unknown toxic effects, including those against microorganisms [17]. A qualification step towards understanding the susceptibility of microorganisms to metal nanoparticles is to consider the cellular mechanisms of the potential antimicrobial effects. Metal nanoparticles interact with microbial cells by multiple biochemical pathways, for example, via the production of reactive oxygen species (ROS) [18]. ROS may result in significant damage to cell structures and can eventually cause cell death [18]. The vulnerability of microorganisms to metal nanoparticles needs to be monitored. For growth-based analysis, common agar diffusion tests, serial dilutions and counting of colony forming units or an endpoint growth determination via turbidity measurements of the cell density are in routine use for evaluating the effects of exposure of nanoparticles on microbial biota, regardless of whether these are desired effects (e.g., against pathogens), or adverse effects on beneficial or environmentally important microorganisms. Commonly used techniques such as agar diffusion tests are frequently hindered by nanoparticle agglomeration or aggregation, and inhibited transport caused by interactions with media components or the solidified agar matrix [19]. As a result of nanoparticle re-aggregation, these tests usually provide inconclusive results or even underestimate nanoparticle toxicity [20].

The antibacterial effect of the prepared nanocomposites was investigated against different microorganisms, namely, Gram-positive (*S. aureus*) and Gram-negative bacteria (*P. aerugenosa*), fungi (*A. niger*) and yeast (*C. albicans*). The antibacterial properties were indicated through observing the formation and diameter of inhibition zone (Fig. 6). The antibacterial effect based on the photocatalytic activity of the modified TiO_2 NBs and the difference in the diameter of the inhibition zone can be attributed to the difference in the cell wall structure.
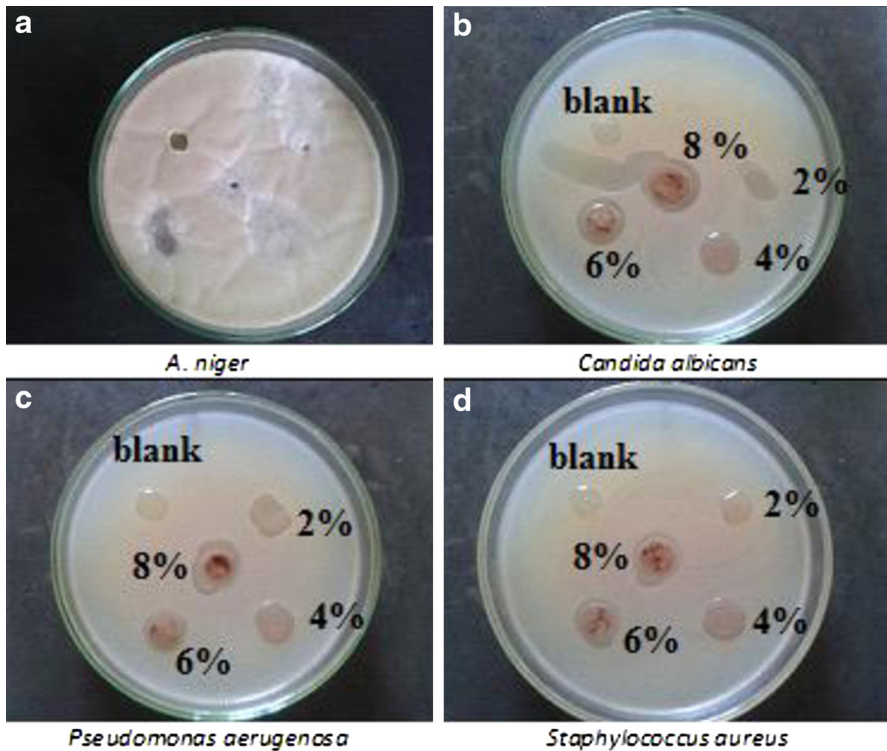
Fig. 6 The antibacterial activity of polymer nanocomposites film containing different concentration of modified TiO$_2$ NBs composites against; **a** fungi (*A. niger*), **b** yeast (*C. albicans*), **c** Gram-negative bacteria (*P. aerugenosa*), and **d** Gram-positive (*S. aureus*)

Conclusion

Polystyrene films were loaded with different ratios of hydrophobic TiO$_2$ nanobelts. The novel modification technique allowed better dispersibility and compatibility of the modified nanobelts in the hydrophobic matrix with large amounts up to 20 %. The tensile strength of the formed films is enhanced significantly along with the elongation at break. Antibacterial properties of the prepared nanocomposites were investigated against four microorganisms and the results revealed good antimicrobial effect for the hydrophobic TiO$_2$ NBs.

References

1. Zhang K, Zheng LL, Zhang XH, Chen X, Yang B (2006) Silica-PMMA core-shell and hollow nanospheres. Collo Surf A Physicochem Eng Asp 277:145–150

2. Kammona O, Kotti K, Kiparissides C, Celis JP, Fransaer J (2009) Synthesis of polymeric and hybrid nano-particles for electroplating applications. Electrochim Acta 54:2450–2457

3. Chen X, Cui ZC, Chen ZM, Zhang K, Lu G, Zhang G, Yang B (2002) The synthesis and characterizations of monodisperse cross-linked polymer microspheres with carboxyl on the surface. Polymer 43:4147–4152

4. Zhang K, Chen HT, Chen X, Chen ZM, Cui ZC, Yang B (2003) Monodisperse silica-polymer coreshell microspheres via surface grafting and emulsion polymerization. Macromol Mater Eng 288:380–385

5. Kumaraswamy G, Dibaj AM, Caruso F (2002) Photonic materials from self-assembly of 'tolerant' core-shell coated colloids. Langmuir 18:4150–4154

6. Song XF, Gao L (2007) Fabrication of hollow hybrid microspheres coated with silica/titania via sol-gel process and enhanced photocatalytic activities. J Phys Chem C 23:8180–8187

7. Jong SP, Jae HK, Young CN, Kown OH (1998) Antibacterial activities of acrylic acid-grafted polypropylene fabric and its metallic salt. J Appl Polym Sci 69:2213–2220

8. Huh MW, Kang IK, LEE DH (2001) Surface characterization and antibacterial activity of chitosangrafted poly(ethylene terephthalate) prepared by plasma glow discharge. J Appl Polym Sci 81:2769–2778

9. Keleher J, Bashant J, Heldt N, Johnson L, Li YZ (2002) Photo-catalytic preparation of silver-coated TiO_2 particles for antibacterial applications. World J Microbiol Biotech 18:133–139

10. Wang Z, Li G, Peng H, Zhang Z (2005) Study on novel antibacterial high-impact polystyrene/TiO_2 nanocomposites. J Mater Sci 40:6433–6438

11. Linsebigler AL, Lu G, Yates JT (1995) Photocatalysis on TiO_2 surfaces: principles, mechanisms, and selected results. Chem Rev 95:735–758

12. Patra N, Salerno M, Cozzoli PD, Athanassiou A (2013) Surfactant-induced thermomechanical and morphological changes in TiO_2-polystyrene nanocomposites. J Coll Interfac Sci 1:103–108

13. Ghanem AF, Williams RL, Abdel Rehim MH, Tian ZR (2014) Tuning a hydrophilic nanobelt's crystal-lattice for interface-tailored nanocompositing with a hydrophobic polymer. J Mater Sci 49:7382–7390

14. Collins CH, Lyne PM (1985) Microbiological methods, 5th edn. Butterworth and Co (Publishers) Ltd. Environ Eng 116(5):805–828

15. Kasuga T, Hiramatsu M, Hoson A, Sekino T, Niihara K (1999) Titania nanotubes prepared by chemical processing. Adv Mater 15:1307–1311

16. Shang SW, Williams JW, Soderholm K-JM (1994) Work of adhesion affects the mechanical properties of silica-filled composites. J Mater Sci 29:2406–2416

17. Marambio-Jones C, Hoek EMV (2010) A review of the antibacterial effects of silver nanomaterials and potential implications for human health and the environment. J Nanoparticle Res 12:1531–1551

18. Su HL, Chou CC, Hung DJ, Lin SH, Pao IC, Lin JH, Huang FL, Dong RX, Lin JJ (2009) The disruption of bacterial membrane integrity through ROS generation induced by nanohybrids of silver and clay. Biomaterials 30:5979–5987

19. Römer I, White TA, Baalousha M, Chipman K, Viant MR, Lead JR (2011) Aggregation and dispersion of silver nanoparticles in exposure media for aquatic toxicity tests. J Chromatogr A 1218:4226–4233

20. Bae E, Park HJ, Lee J, Kim Y, Yoon J, Park K, Choi K, Yi J (2010) Bacterial cytotoxicity of the silver nanoparticle related to physicochemical metrics and agglomeration properties. Env Toxicol Chem 29:2154–2160